

Design of a Wheelchair with Legs for People with Motor Disabilities

Parris Wellman, Venkat Krovi, Vijay Kumar, and William Harwin

Abstract—A proof-of-concept prototype wheelchair with legs for people with motor disabilities is proposed, with the objective of demonstrating the feasibility of a completely new approach to mobility. Our prototype system consists of a chair equipped with wheels and legs, and is capable of traversing uneven terrain and circumventing obstacles. The important design considerations, the system design and analysis, and an experimental prototype of a chair are discussed. The results from the analysis and experimentation show the feasibility of the proposed concept and its advantages.

I. INTRODUCTION

MOTORIZED WHEELCHAIRS with sophisticated controls are available for people with disabilities. While they can locomote on prepared surfaces most are unable to surmount common obstacles like steps and curbs. (See ANSI/RESNA WC/10 or ISO 7176/10 standards for determination of the obstacle climbing ability of a wheelchair). Architectural modifications such as curb cuts, ramps and elevators improve accessibility but are primarily limited to new buildings. Wheelchair users often cannot enjoy strolling on beaches nor can they easily cross muddy patches and potholes. Previous research in rehabilitation engineering has concentrated primarily on constructing a better wheelchair (see [9], [15], [17], [23]). Many special purpose aids [10], [19], [21] including stair climbers [22] and customized outdoor buggies [9] have been developed to solve specific problems but they tend to be customized to a particular environment and are not versatile. See Table I for a brief survey of available solutions.

A legged vehicle allows locomotion in environments cluttered with obstacles where wheeled or tracked vehicles cannot be used. It is inherently omni-directional, provides superior mobility in difficult terrain or soil conditions (sand, clay, gravel, rocks, etc.) and provides an active suspension. The legs also give the chair versatility and allow it to be re-configured. When stationary, one of the legs can be used as a manipulator

Manuscript received November 22, 1994; revised July 12, 1995. This work was supported in part by the the Whitaker Foundation and also supported in part by the NSF under Grants MSS-9157156, MIP-9420397, and CISE/CDA 88-22719, the Nemours Foundation, and the University of Pennsylvania Research Foundation.

P. Wellman and V. Krovi are with the Department of Mechanical Engineering, GRASP Laboratory, University of Pennsylvania, Philadelphia, PA 19104 USA.

V. Kumar is with the Department of Mechanical Engineering, GRASP Laboratory, University of Pennsylvania, Philadelphia, PA 19104 USA. He is also with the Applied Science and Engineering Laboratories, A. I. duPont Institute, Nemours Foundation, Wilmington, DE USA.

W. Harwin is with the Applied Science and Engineering Laboratories, A. I. duPont Institute, Nemours Foundation, Wilmington, DE USA.
IEEE Log Number 9414592.

TABLE I
A SURVEY OF AVAILABLE METHODS (TECHNOLOGY) FOR ENHANCING MOBILITY

SOLUTION	ADVANTAGES	DISADVANTAGES
Architectural modifications (curb cuts, ramps, accessible elevators)	Usually low cost to consumers. Assists all ages and abilities. Often a simple technology with low maintenance. High consumer acceptance.	Regulations do not apply to private or historic buildings. Apply only in limited measures to apartment buildings. Many buildings do not comply with the law. Not applicable in most outdoor settings.
Transfer technologies	Can transfer to the vehicle most appropriate for the environment.	May require assistance with a transfer.
Stair climbing wheelchairs	Allow access to certain wheelchair inaccessible environments.	Does not generalize to other environments, does not work on all types of stairs, often a bulky addition to the wheelchair, slow to deploy, poor maintenance.
Customized chairs (out door buggies) Curb climbers	Optimized for the environment. Low cost. For example, golf carts, outdoor chairs and special purpose sand buggies.	Requires transfer. Suitable for only small obstacles, due to power limitations of the wheelchair.

in order to perform simple tasks such as reaching for objects or pushing open doors.

In the past two decades, several articulated legged vehicles have been designed and built in research laboratories. Most work has focused on *statically stable* locomotion, characteristic of insects [27], in which the legs maintain the vehicle in static equilibrium. This is contrasted with *dynamically stable locomotion* [13], [18] that is exhibited by galloping four-legged animals and walking (or running) humans. A number of proof-of-concept statically stable legged robots have been built. These have been four-legged [5], [14] or six-legged [16], [24]. Dynamically stable legged systems including bipeds and quadrupeds have also been built and studied [13], [18]. Given the current state of technology, they are less reliable than their statically stable counterparts and hence not suitable for the application considered here.

Actively controlled articulated wheeled vehicles possess many of the advantages of legged vehicles. A three-module vehicle with six wheels for planetary exploration is described in [11] and a similar system has been proposed for inspection and maintenance operations in nuclear plants in [6]. However, these vehicles cannot be considered as a viable alternative to motorized wheelchairs because of their configuration and size.

Much of the previous work in this area has been focused on unmanned operation and intelligent vehicle systems. In contrast, mobility aids for people with disabilities must be designed to exploit the capabilities of the human operator. While a human is not very good at performing low-level coordination tasks, he/she is extremely adept at high-level decision making. For example, sequencing of the legs and optimal placement of feet based on stability criteria are tasks which require computation and are difficult to perform manually [11]. On the other hand, a human will excel at the fairly complex

task of surveying the terrain and planning an approximate path based on minimal information.

In this paper, a proof-of-concept prototype wheelchair with legs for people with motor disabilities is proposed. The main objective is to demonstrate the feasibility of a completely new approach to mobility for the motor disabled. The important design considerations, the system design and an experimental prototype are discussed. Preliminary experimental results and future research directions are also presented.

II. CONFIGURATION DESIGN

A primary consideration in designing rehabilitation aids is safety. Because, statically stable machines are more reliable and are likely to be more acceptable to consumers than dynamically stable machines, we restricted ourselves to statically stable locomotion. The design considerations for statically stable, legged vehicles are well known [11], [16], [24], [28]. The vehicle must have at least four legs for statically stable locomotion. As the number of legs increases, the stability of the vehicle and its reliability increases at the cost of increased complexity, weight and cost. A four-legged vehicle is capable of climbing steps and stairs, crossing ditches and stepping over obstacles. Thus a four-legged vehicle with a fifth leg to act as a safety crutch is an attractive proposition. The disadvantage with the design is that it is difficult to achieve the required strength/weight ratio. With a payload of 100 kgs, if we assume a maximum vehicle weight of as much as 100 kgs (net weight = 200 kgs), each leg must be able to support a minimum of 100 kgs (in addition to providing the tractive force). This translates to a payload/weight ratio of over 4 for each leg. It is difficult to design a moderately expensive, compact actuation system with such stringent requirements. By increasing the number of legs, the required strength/weight ratio becomes smaller but the design becomes less compact. Further, our informal survey of potential consumers indicated that a four-legged walking chair (e.g., [33]) is likely to suffer from a lack of acceptance by consumers.

In a conventional wheeled system the payload is supported passively while the actuation system only has to provide the tractive force. Motivated by this observation we considered an alternative design that combines the advantages of legged locomotion (versatility, adaptability) with wheeled locomotion (reliability, superior stability). An example of such a *hybrid* vehicle with four wheels (two powered) and two legs is shown in Fig. 1. A hybrid chair would be capable of using powered wheels to navigate on a flat surface. The legs would be used primarily on uneven terrain and on unprepared surfaces. A maneuver similar to walking is accomplished by using the legs to drag the vehicle forward or backward as shown in Fig. 2. The legs can be used with the wheels to provide additional traction on slippery surfaces. They can also be used as manipulators to push open doors, reach for objects, move aside obstacles or open doors. The legs and wheels can be employed to climb steps or curbs using the six-step procedure shown in Fig. 3. Note that the wheels must either be powered or be equipped with brakes so that the transition from stage 2 to stage 3 is accomplished safely. If the wheels are powered (as

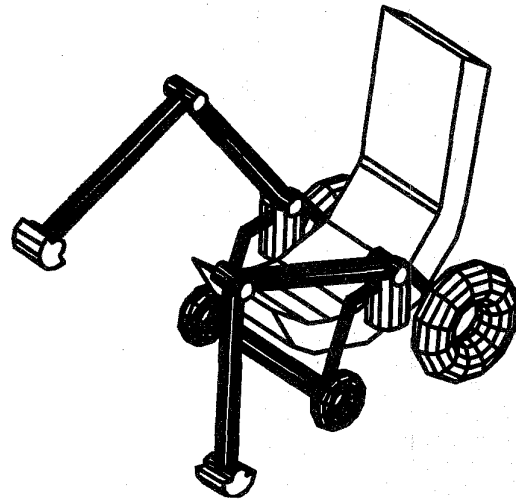


Fig. 1. An artists conception of a hybrid vehicle with two legs/manipulators.

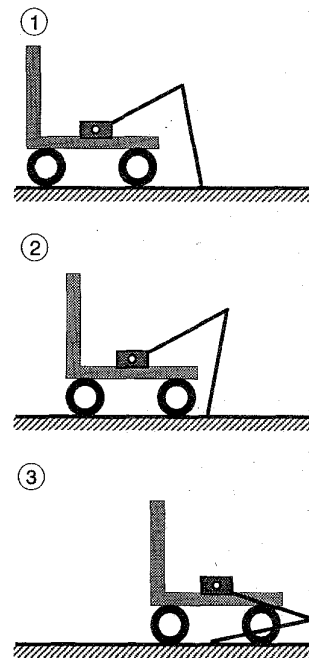


Fig. 2. Locomotion by "walking."

are the legs), the system is redundantly actuated. This allows us optimize the locomotion as discussed in [11], [25]. The legs can be used to step over small obstacles (rocks, toys, potholes) or avoid areas with poor support or traction as seen in Fig. 4. Finally, a design that includes wheels would be more acceptable to consumers (than a design for a walking vehicle) because of the emphasis on using wheels as primary locomotion elements.

Unlike a legged system, the hybrid vehicle cannot locomote without wheels nor can it move with a uniform velocity over an unprepared surface. However, it can accomplish most statically stable four-legged maneuvers by decomposing them into steps that involve maneuvering of one leg at a time. Thus the reduced complexity, lower cost and improved reliability

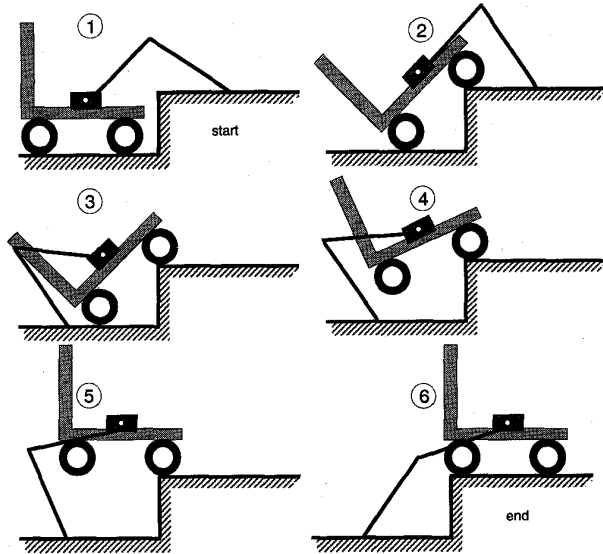


Fig. 3. Complete step climbing maneuver.

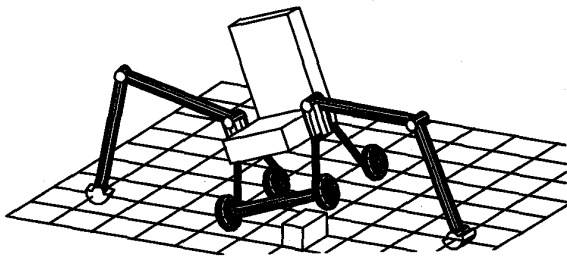


Fig. 4. Stepping over an obstacle.

and safety are at the expense of some loss in mobility. For example, stair climbing is a difficult task. Although it is not considered in this paper, if it is seen to be an important task, additional legs can be added (at the risk of increasing its complexity) to achieve this objective. Thus, the hybrid chair is still quite versatile and has many desirable features that conventional wheelchairs and special purpose locomotion aids do not possess. We note that a similar vehicle with wheels attached to articulated legs is proposed for forestry work in [5].

III. OPTIMIZATION OF THE VEHICLE GEOMETRY

It is necessary to establish performance objectives and design ranges for the optimization of the vehicle. Because our main goal is to demonstrate the feasibility and viability of the hybrid mobility system, instead of attempting to strictly adhere to existing wheelchair standards, we set for ourselves the following performance objectives for a proof-of-concept prototype.

- The mobility system must be able to climb a 12 in high step (an informal survey of the city of Philadelphia led us to the conclusion that this should be as much mobility as is required in most situations).
- It must be less than 30 in (0.76 m) wide (the width of standard doorways in the University of Pennsylvania).

- It should be light in weight. 70 lbs or 32 kgs (without payload and batteries) is a realistic upper limit.
- It should be as compact as possible [wheelbase less than 30 in (0.76 m), leg length less than 40 in (1.02 m)].
- The range should be as great as possible (which implies minimizing the motor torque and power requirements).
- It must rely on proven sources of power (such as lead acid batteries and electric motors).

The above criteria provide for the design of a highly mobile vehicle that has the capacity to traverse difficult terrain. Note that such a vehicle may not possess the ability to climb stairs. Further, in order to provide the mobility system with maximum flexibility, it made sense to make the design as close to completely symmetric (both front to rear and side to side) as possible (else, we risk the situation of having designed a vehicle which is able to climb onto higher obstacles than it is able to climb down from).

Central to the design of the system are the versatility and the strength to weight ratio of each leg/manipulator. Many leg designs were explored (see, for example, [25]) and discarded because they scaled poorly, or were not sufficiently versatile, or proved too cumbersome to package. We finally adopted a design in which each leg has three revolute joints. The detailed design can be seen in Fig. 9. The axis of the first joint is vertical (not shown shown in the figure). The next two joint axes are horizontal and parallel. They are driven through a parallel-drive actuation scheme. This allows us to place all the motors on the chassis (base) and the system requires less power and lower actuator torques [20].

Accepting the general configuration shown in Fig. 1 and the need to perform the maneuvers shown in Figs. 2-4, the next step of determining the critical dimensions and sizing the actuators for the parallel-drive leg design can be addressed. Because the weight and size of a DC motor increases rapidly for large torque ratings it is meaningful to size the system so that the smallest possible actuators can be employed. Because the step climbing maneuver shown in Fig. 3 requires the largest leg forces and actuator torques, we optimize the system so that the peak motor torques required in the step climbing maneuver are minimized. Further, because the maneuver can be reduced to a two-dimensional (planar) task (as shown in Fig. 3), it is sufficient to consider two two-degree-of-freedom legs.

In Fig. 5 we define the relevant design variables. r is the radius of the wheel, h is the height of the first joint of the leg above the center line of the wheels, w is the wheel base of the chair, c is the horizontal distance from the center of the front wheel to the foot at the beginning of the maneuver and l is the length of each link of the leg. The height of the obstacle is given by q . In order to make the chair symmetric, the manipulator is assumed to be attached at the midpoint of the wheel base. The link lengths were chosen to be equal in order to maximize the workspace of the manipulators and therefore, their mobility and versatility. The center of mass is located within the chair at a distance m from the center of the rear hub and at an angle β from the line joining the two centers as shown in the figure. We define a and b to be multipliers between 0 and 1, so that bh is the height of the center of mass and aw is the distance of the center of mass from the rear hub

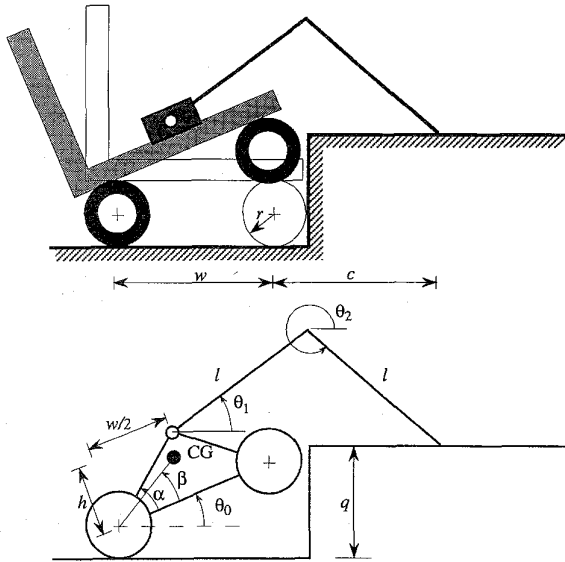


Fig. 5. The different parameters for the wheelchair.

along the wheelbase. Therefore, in Fig. 5,

$$\tan \alpha = \frac{2h}{w}, \quad \tan \beta = \frac{bh}{aw}, \quad m = \sqrt{(aw)^2 + (bh)^2}.$$

Obviously, from symmetry considerations, $a = 0.5$ is desirable. From the point of view of stability, b should be made as small as possible. Because the parameters a and b are determined by the mechanical design, they are held constant during the optimization.

In the optimization exercise we use statics to model the vehicle during the step climbing maneuver. This is a reasonable assumption because the vehicle movements will be quite slow. In Fig. 5, the foot force F required to maintain the vehicle in static equilibrium is:

$$F = \frac{Wm \cos(\theta_0 + \beta)}{\frac{w}{2 \cos \alpha} \cos(\theta_0 + \alpha) + l \cos \theta_1 + l \cos \theta_2} \quad (1)$$

where W is the weight of the vehicle. The actuator torques required to exert this force are given by

$$\tau_1 = Fl \cos \theta_1 \quad (2)$$

$$\tau_2 = Fl \cos \theta_2. \quad (3)$$

If the entire step climbing maneuver is parameterized by a single variable, s , varying from 0–1, such that all the displacement variables (e.g., $\theta_0, \theta_1, \theta_2$) are functions of s , the variation of the joint torques can be written as a function of this variable. Thus if the motor sizes are to be minimized, the objective is to minimize the maximum joint torque:

$$\min_{\mathbf{X}} [\max_{i=1,2} \{|\tau_1(s)|, |\tau_2(s)|, 0 \leq s \leq 1\}] \quad (4)$$

where $\mathbf{X} = [l, h, w, r, c]^T$.

There are three key constraints on the design variables. First,

$$\left(c + 2r + \frac{w}{2}\right)^2 + (q + r + h)^2 - (2l)^2 \leq 0. \quad (5)$$

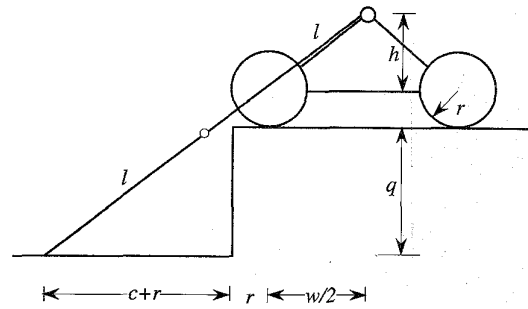


Fig. 6. The mobility constraint.

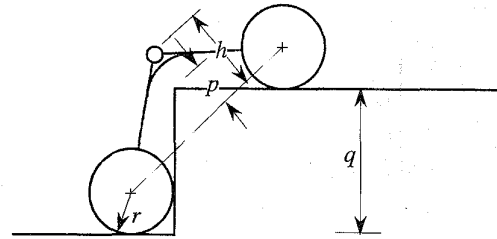


Fig. 7. The clearance constraint.

Equation (5) defines a *mobility constraint*, the derivation of which can be seen quite clearly in Fig. 6. It simply ensures that the manipulator links are adequately long to provide the full range of motion required. Note that we have assumed that the maneuver is symmetric in the sense that the parameter c is the same for lifting the rear onto the curb as it is for lifting the front.

In addition, we have a *stability constraint* that prevents the vehicle from overturning as it crosses obstacles (see Fig. 5):

$$\theta_0 + \beta - \frac{\pi}{2} \leq 0$$

or,

$$\sin^{-1}\left(\frac{q}{w}\right) + \beta - \frac{\pi}{2} \leq 0. \quad (6)$$

It worth noting that this constraint addresses static stability. The analysis of stability during motion (see for example, [1]) is beyond the scope of this paper.

Fig. 7 shows the definition of (7), the *clearance constraint*, which ensures that there is enough clearance between the bottom of the vehicle and the obstacle to be crossed. Here p , the penetration of the step into the line joining the hubs should not exceed h :

$$h - \frac{(q-r)\sqrt{w^2 - q^2} - qr}{w} \geq 0. \quad (7)$$

In addition, the following limits (all dimensions in inches) were chosen for the optimization variables:

$$3 \leq c - r \quad (8.1)$$

$$7.5 \leq h \quad (8.2)$$

$$l \leq 20 \quad (8.3)$$

$$w \leq 30 \quad (8.4)$$

$$3 \leq r. \quad (8.5)$$

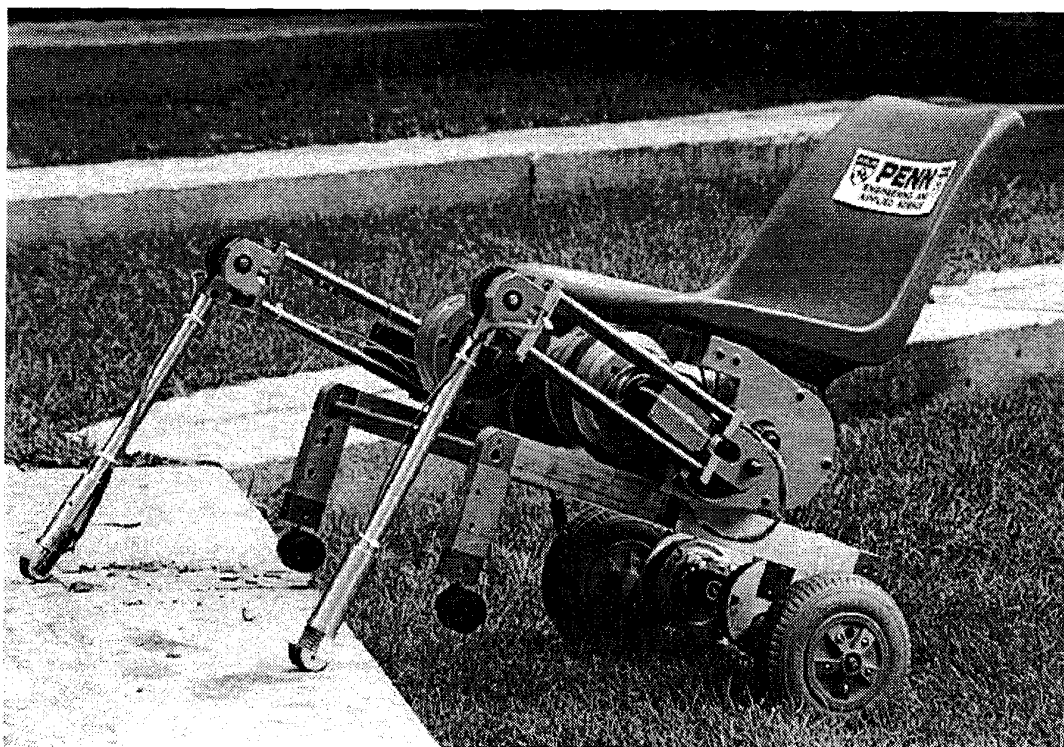


Fig. 8. The prototype of the wheelchair based on the optimal design parameters.

TABLE II
OPTIMAL DESIGN PARAMETERS

	Preliminary prototype [26]	Optimal parameters (see Figure 8)
Weight	77.0 lb. (34.9 kg)	62.0 lb. (28.2 kg.)
Width	32.0 in (0.81 m)	28.0 in (0.71 m)
w	28.0 in (0.711 m)	21.0 in (0.53 m)
r	3.5 in (0.089 m)	3 in (0.076 m)
l_1	25.5 in (0.648 m)	15.9 in (0.404 m)
l_2	25.0 in (0.635 m)	15.9 in (0.404 m)
h	22.0 in (0.559 m)	7.5 in (0.190 m)

The limit on c is to ensure that the leg foothold is not at the edge of the step. The lower limit on h arises from mechanical design considerations. r is restricted because the smallest off-the-shelf wheel is 3 in (0.076 m) in radius. Finally, the curb height q is set to a foot (0.3048 m).

A nonlinear programming routine in the Matlab™ optimization tool box was used to determine the optimal parameters with the results shown in Table II.

IV. THE EXPERIMENTAL PROTOTYPE

A. Mechanical Design

A picture of the prototype is shown in Fig. 8 while the essential mechanical details are shown in Fig. 9. Note that the legs in the prototype do not possess the third degree of freedom (described in Section III) that is required for such three-dimensional maneuvers as the one shown in Fig. 4. The two 12 V batteries, the amplifiers and the controller are not shown

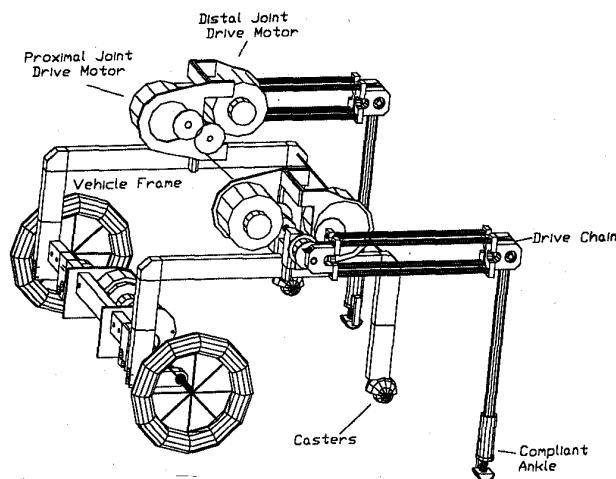


Fig. 9. The chassis with four wheels and two legs.

in the figure. The prototype as shown in Fig. 8 weighs 62 lbs (28.2 kgs), not including the controller and batteries. There are only two design changes from the optimal parameters in Table II. Although the optimal link length for each link is 15.9 in, a compliant ankle is attached to the distal link making it 3 in longer (total length 0.48 m) than the proximal link. Second, the smallest wheel that could be purchased off the shelf (with the desired load rating) had a radius of 4.5 in (0.114 m).

Each leg has a reach of approximately 32 inches (0.81 m). The proximal link is made from four thin walled titanium tubes. This arrangement allows for high stiffness in torsion and in bending with a very small penalty in weight. Power

is transmitted to the distal link through a chain and sprocket transmission. The chain is preloaded to remove backlash. The proximal link is designed so that the chain passes through the neutral axis of the link to minimize bending moments so that the link is in pure compression. The tension in the chain is sensed by strain gages on the proximal link and this allows the measurement of the transverse foot force. The distal link is fabricated from an aluminum tube. At the end, it is equipped with a compliant ankle which is a linear, spring-loaded joint on linear bearings. The ankle is instrumented with a linear potentiometer that enables the estimation of the axial foot force.

Each joint in the leg is driven with a single DC gear motor (PMI 12FG) capable of exerting 200 in-lbs. (22.6 N-m) of torque at 26 rpm, with a peak (stall) torque of 240 in-lbs. (27.12 N-m). Another reduction of 3:1 is accomplished between the gear motor and the joint. The maximum foot force that can be exerted continuously is 37.5 lbs (166 N), with a peak rating of 45 lbs (200 N). Each rear wheel is also driven by a similar gear motor (PMI 9FG) with a rating of 40 in-lbs. (4.5 N-m) of continuous torque. The maximum foot speed is approximately 2.2 ms. At the rated wheel speed (78 rpm), the chair moves at 0.93 meters/second (3.4 km/h). All motors (legs and wheels) are mounted on the chassis (base of the chair) so that their weight is not borne by the moving links.

B. Control System

The motors are driven by 20 kHz PWM switching amplifiers (Kollmorgen Industrial Drives VXA 48-8-8) that operate off of a 24 V dc source. Although in the laboratory we use transformers and ac line voltage, the vehicle can be operated on two standard 12 volt lead acid batteries. The peak current drawn is 6 A. The amplifiers are configured to clamp to the motor current determined by the control signals received from the control computer. System feedback is accomplished through 500 line resolution incremental optical encoders also supplied by Kollmorgen/PMI. Because of the gearing, the encoders provide a resolution of 2500 counts per degree of joint shaft rotation for each leg. Position is measured directly from the encoders that are mounted on the input side of each motor and the velocity is computed digitally by taking successive derivatives of the position signal. A digital I/O card (Keithley Metrabyte DDA 06) is used for data acquisition. In addition, as mentioned earlier, both components of foot forces are available for feedback. The circuitry for conditioning and amplifying strain gage signals (Analog devices, 3B18) is mounted on the distal link close to the strain gages to minimize noise. A data acquisition card (Real Time Devices, ADA2000) is used to convert the analog strain measurements and the ankle displacements into digital signals.

The control computer is an IBM compatible 486 machine with an i860 coprocessor running concurrently. The i860 is used to perform the control computations that are necessary to process the sensory data and coordinate the multiple actuators. The 486 processor performs all system input and output tasks. This includes nonsynchronized tasks such as reading and writing to files, processing input from the user, and controlling

the video display which are performed in the background, as well as synchronized tasks such as reading the encoders, providing input data to the i860 and sending control signals to the motors. A shared memory block is used to facilitate exchange of information between the two processors.

C. Control Algorithm

The control algorithm employed for a single leg is an impedance control scheme [8] running at 500 Hertz and is similar to control algorithms conventionally used for robot manipulators. The dynamics of a single leg can be written as

$$\mathbf{H}(\theta)\ddot{\theta} + \mathbf{h}(\theta, \dot{\theta}) + \mathbf{g}(\theta) = \tau - \mathbf{J}^T \mathbf{F} \quad (9)$$

where \mathbf{H} is the $n \times n$ inertia matrix for the articulated leg linkage, n is the number of degrees of freedom (in this case, joints), θ is the $n \times 1$ vector of joint angles that completely describe the leg configuration, $\dot{\theta}$ and $\ddot{\theta}$ are the corresponding velocities and accelerations respectively, \mathbf{h} is the $n \times 1$ vector of inertial terms that are nonlinear functions of the velocities, \mathbf{g} is the $n \times 1$ vector of gravitational terms, τ is the $n \times 1$ vector of actuator torques, \mathbf{J} is the $n \times n$ Jacobian matrix and \mathbf{F} is the $n \times 1$ vector of components of the force exerted by the leg on the ground. For planar motion, $n = 2$. The leg has two joints (and therefore two actuators) and there are two components of leg force if we assume a point contact with friction.

If \mathbf{x} is the Cartesian position of the foot (actually the contact point on the foot), a $n \times 1$ vector, it is a function of the joint angles and we can write this as a function:

$$\mathbf{x} = \mathbf{f}(\theta). \quad (10)$$

According to Hogan's impedance control scheme [8], the leg is controlled to behave like a target impedance. We choose this impedance to be linear:

$$\mathbf{M}\ddot{\mathbf{x}} + \mathbf{C}(\dot{\mathbf{x}} - \dot{\mathbf{x}}^d) + \mathbf{K}(\mathbf{x} - \mathbf{x}^d) = \mathbf{F} - \mathbf{F}^d \quad (11)$$

where \mathbf{M} , \mathbf{C} , and \mathbf{K} are the desired $n \times n$ mass, damping and inertia matrices, and the superscript "d" indicates the desired trajectory and force. If this behavior is achieved, the leg end-point deviates from the trajectory \mathbf{x}^d and the force \mathbf{F}^d according to (11). If the desired task is to contact a specific point on the ground with a specified force (in the horizontal and vertical direction), the desired velocity is set to be zero and the desired position and force are the specified quantities. It is desirable to choose the target impedance so that it is suitably mismatched with the impedance of the contacting surface. Thus, broadly speaking, a stiff ground would dictate a target stiffness that is low, while a high target stiffness would be better suited to a soft ground. On the other hand, if the desired task is to move through free space along a specified trajectory, the desired force would be zero and the target impedance would be chosen to be very stiff.

From (9)–(11), the control law that is required to implement the target impedance behavior, is derived

$$\begin{aligned} \tau = & [\mathbf{H}\mathbf{J}^{-1}\mathbf{M}^{-1} + \mathbf{J}^T](\mathbf{F} - \mathbf{F}^d) \\ & + [\mathbf{g} - \mathbf{H}\mathbf{J}^{-1}\mathbf{M}^{-1}\mathbf{K}(\mathbf{f}(\theta) - \mathbf{f}(\theta^d))] \\ & + [-\mathbf{H}\mathbf{J}^{-1}(\mathbf{M}^{-1}\mathbf{C}\mathbf{J}(\dot{\theta} - \dot{\theta}^d) + \dot{\mathbf{J}}\dot{\theta}) + \mathbf{h}]. \quad (12) \end{aligned}$$

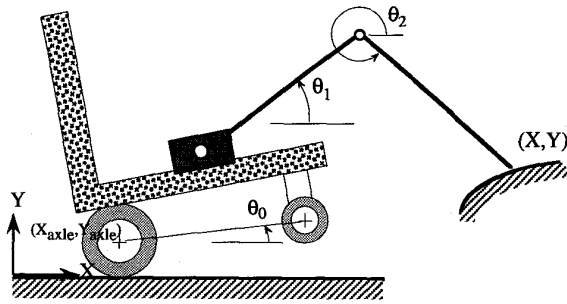


Fig. 10. Definitions of symbols in the experimental plots.

This requires an estimate of the different inertial parameters. However, because in the prototype system, the gearing ratio is very high (450:1 in the leg motors), the friction in the gears dominates and modeling errors do not adversely affect the performance. In fact, it has been our experience [26] that assuming H to be proportional to an identity matrix and setting h and other nonlinear velocity terms to be zero produces satisfactory performance, while enabling higher sampling rates.

V. PRELIMINARY TESTS AND EXPERIMENTAL RESULTS

The results of several experiments are presented here. The objective is to convey a sense of the capabilities of the experimental system and some idea of the dynamic performance. The symbols used in the plots in this section are shown in Fig. 10.

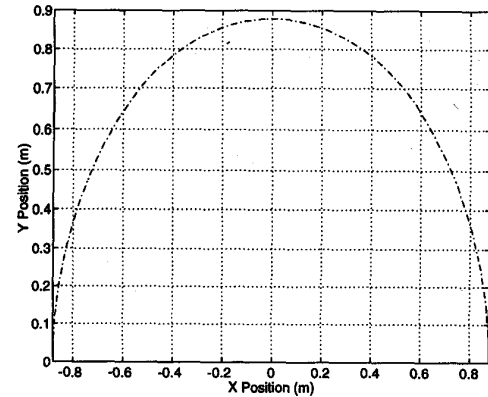
A. Movement Through Free Space

While not supporting or propelling the vehicle, it is necessary for the leg or manipulator to move quickly from one position to another. In this experiment the leg was commanded to move from a position all the way in front of the vehicle to all the way to the back. Essentially, the controller is given step inputs of 180 degrees for both joints. While the motion is not coordinated, the objective of this experiment is to demonstrate the peak velocities during reaching maneuvers.

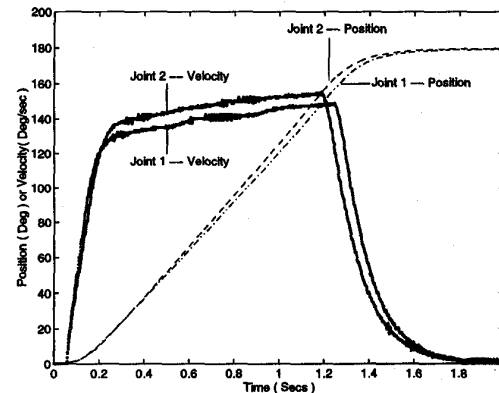
The trajectory of the foot is shown in Fig. 11(a). The joint motion is shown in Fig. 11(b), while the y -component of the Cartesian motion of the foot is shown in Fig. 11(c). The velocity is obtained from the position data using a simple backward difference scheme and is shown unfiltered. The peak foot velocity (when not loaded) is approximately 2.2 m/s and the leg can move from one extreme point in its workspace to the other extreme in 1.75 s. These are indicative of the performance during reaching maneuvers and when changing the footholds (support points).

B. "Walking" on Level Ground

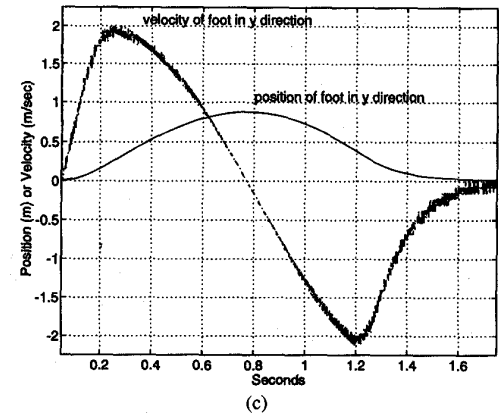
The proposed system can use its legs to propel (drag) the chair even when the wheels are not powered as shown in Fig. 2. We conducted experiments on this walking-like maneuver with a 150 lbs (68.2 kgs) subject. The foot trajectories and joint movements for a typical experiment are shown in Fig. 12. Note



(a)



(b)



(c)

Fig. 11. Leg movement through free space: (a) the trajectory of the foot in Cartesian space; (b) the joint displacements and velocities; and (c) the y -component of the Cartesian position and velocity.

that the wheel motors are not used during this maneuver, and therefore, all the tractive forces are provided by the leg.

The ideal motion (solid line) and actual motion (dashed line) of the foot relative to the vehicle is shown in Fig. 12(a). The ideal motion is a rectangle of 4 inches (0.1 m) height to avoid small obstacles on the ground with a stride of 20 inches (0.5 m). AB is the phase in which the vehicle is propelled forward while BC (lift-off), CD (transfer) and DA (landing) are the three phases during return. The actual motion of the foot, shown dashed, approximates the rectangle. It is different from

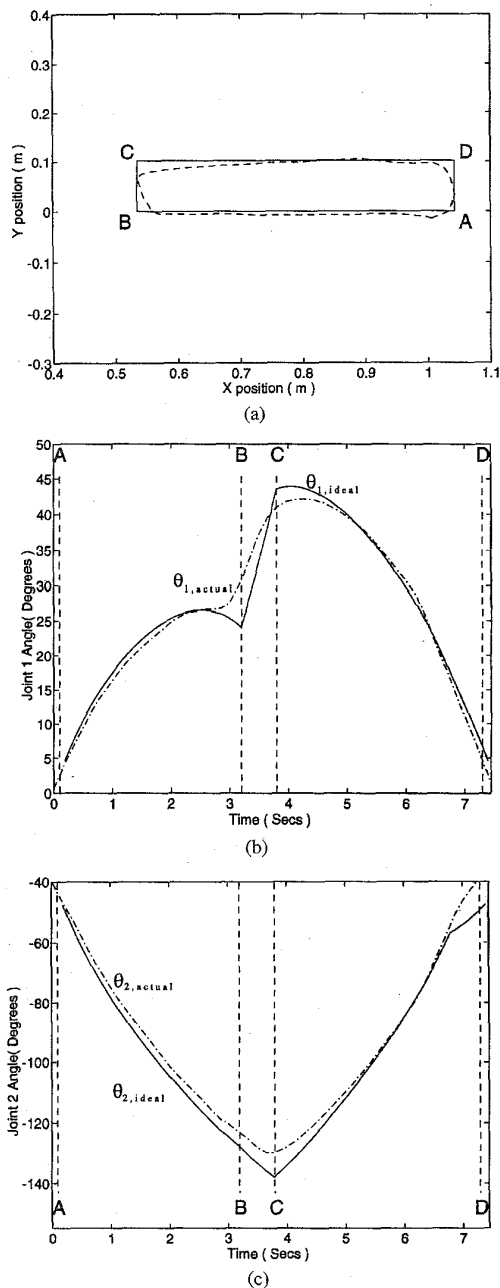


Fig. 12. A cycle of leg movement during the "walking" maneuver: (a) Cartesian motion of the foot; (b) Joint 1 position; and (c) Joint 2 position.

the solid line for two reasons. First, the desired motion (not shown) is the rectangle with the corners rounded off. Second, the deformations of the compliant ankle are not incorporated into the plots. Because during the propelling phase, the vehicle weight causes the ankle to deform, the dashed line is in fact below the solid line. During the lift off (BC) and landing stages (DA), the dynamics of the ankle (a spring-mass system) are significant. (These deformations are not fed back to the controller and the data acquisition system. Only the estimated axial forces are used by the controller.) The joint motions (ideal and actual) are shown in Fig. 12(b) and (c).

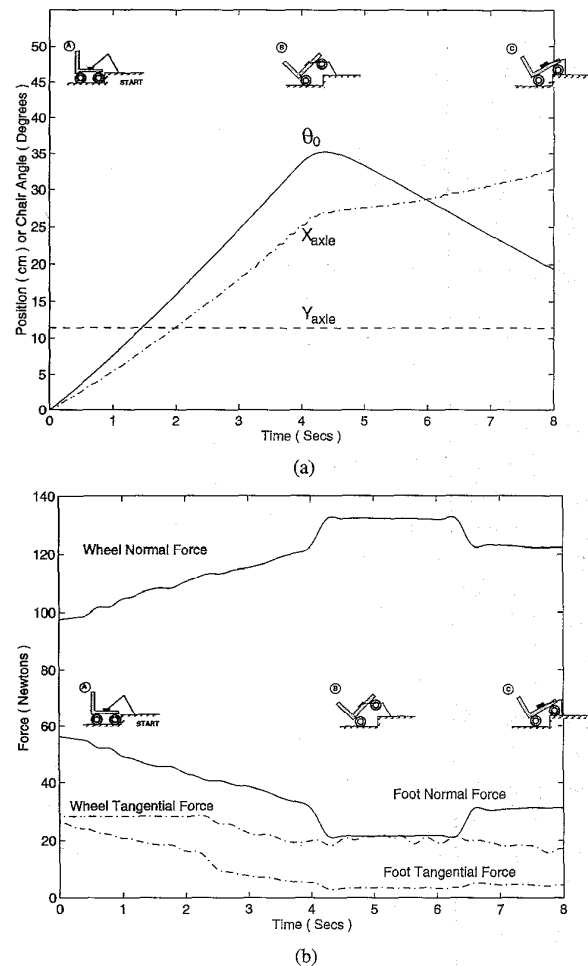


Fig. 13. A step climbing maneuver: (a) the position of the axle (forward movement of the chair) and the inclination (θ_0) of the chair; and (b) the wheel and foot forces.

C. Step Climbing Maneuver

The results of a step climbing maneuver are shown in Fig. 13. The 8 s time history corresponds to half the maneuver shown in Fig. 3. The payload is zero in this experiment and therefore, the net weight is approximately 70 lbs. The chair is initially horizontal and the legs are positioned on the curb (stage A in Fig. 13). Then the front wheels are lifted and moved up and over toward the curb (stage B). The vertical lift is a little higher than the curb height of 12 inches. Then the chair is moved forward while lowering the front wheel onto the curb (stage C).

The chair angle, θ_0 , and the rear axle position (see Fig. 10 for definitions) are shown in Fig. 13(a), while the foot forces are shown in Fig. 13(b). The chair tilts back to a peak value of 37° (stage B). (This is a worst case scenario because, as shown in the next section, the maximum required tilt angle for a 12 in step is less than 25° .) Note that the chair is constantly moving forward during this maneuver. The foot forces are the highest when the maneuver starts. As the tilt of the chair increases, the foot forces drop as expected (phase A \rightarrow B). When the chair is lowered (phase B \rightarrow C), θ_0 decreases and the foot forces

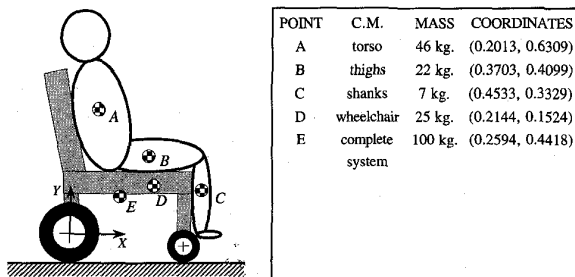


Fig. 14. The coordinates of the centers of mass of the ISO dummy and the wheelchair. (All dimensions are in meters and the coordinates are with respect to the reference frame attached to the rear wheel axle.)

again increase. However, this is not reflected in the normal component of the foot force in Fig. 13(b). This is because our force sensors show considerable hysteresis at high loads (over 125 Newtons), when the spring coils get jammed against their bearings. Note that the wheels are active during this maneuver. The wheel tangential force is at its maximum of 30 N. (A software limit on the wheel torque bounds it below 3.5 N-m.) Finally the friction in the system is easily seen from the initial tractive force (over 50 N) required to move the system.

A more detailed discussion of the foot forces requires some explanation of how the desired foot forces are generated. When the arms are used to support the vehicle or propel it forward, it is necessary to maintain the contact forces at a level that prevents slippage and at the same time, prevent the contact forces from becoming excessively large. Since our configuration design has redundant actuation, we can optimize the force distribution. An active traction optimization scheme [25], [26] ensures that the ratio of the tangential foot force to normal foot force never exceeds a suitable threshold. This explains why the normal foot forces and tangential foot forces are roughly proportional to each other.

VI. ANALYSIS OF THE CHAIR WITH AN OCCUPANT

The main objective of this section is to present an analysis of the curb-climbing maneuver with a payload to demonstrate feasibility. We consider a 75 kg rider, an ISO dummy (ANSI/RESNA WC/11 or ISO 7176-11 standard), riding in our chair and using the legs to climb a 1 foot (0.3048 meters) curb as shown in Fig. 3. The centers of mass of the torso, legs and the wheelchair, and the appropriate masses, are shown in Fig. 14. A computer simulation of the dynamics of the system was used to analyze the stability of the system and the motor torques encountered during the maneuver. The results of the maneuver are shown in Fig. 16. Actually only half the maneuver (the lifting of the front wheels of the chair) is shown here to keep the discussion short. (It is during stages 1–2 (see Fig. 3) that the tilt angle of the chair is at its highest and the stability is the poorest.) The trajectory of the chair is assumed to be a kinematically smooth curve starting from stage 1 and ending at stage 2 (in Fig. 3). It is assumed that this part of the maneuver is accomplished in 5 seconds. Finally we again assume for this analysis that the system is symmetric. Thus in what follows, we show the results for only one side (1 leg and 1 wheel).

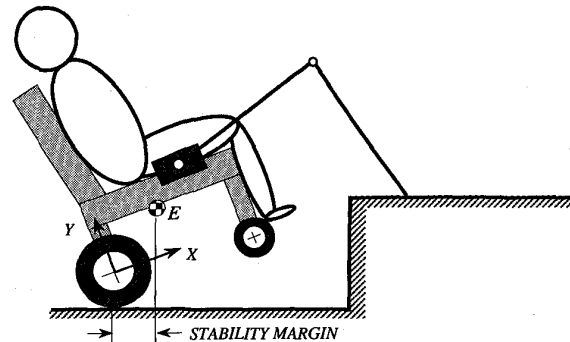


Fig. 15. The definition of the stability margin.

In order to quantify the stability of the system, we define a measure of static stability, called the stability margin, according to Fig. 15. It is a variant of what is used in legged systems [5], [24], [28]. When the center of mass of the wheelchair-rider system falls within the support polygon defined by the contact points between the wheels and the ground or the legs and the ground, the vehicle is statically stable. In the planar model of the chair-rider system shown below, the stability margin measures the distance from the projection of the center of mass of the entire system on the ground to the nearest support point. Clearly, if the stability margin is positive, the system is statically stable.

In the simulation, the maximum tilt of the chair is established to be less than 25° for a one foot curb. See Fig. 16(a). In contrast to manual wheelchairs where the maximum allowable tilt angle is substantially smaller [2], because the active coordination of the powered wheels and legs prevents slip and the prototype has a much lower center of gravity, much higher tilt angles can be achieved. The stability margin is seen to be positive throughout the maneuver. As seen in Fig. 16(b), the peak torques for the leg joints occur at the beginning of the maneuver and are well below the maximum continuous torque of 67.8 Newton-meters that can be achieved by our motors. The foot and wheel forces are shown in Fig. 16(c). Note that the maximum foot force is well below the maximum of 200 Newtons. It should also be noted that the maximum foot forces and leg torques occur at the beginning of the maneuver (stage 1 \rightarrow 2 in Fig. 3). The torques during stages 3–6 (Fig. 3) are always lower than these levels.

VII. DISCUSSION

It is important while designing rehabilitation aids to incorporate feedback from consumers during the design process. We obtained this input by consulting consumer designers at the Applied Science and Engineering Laboratories, A. I. duPont Institute. (The consumer designers are people who can benefit from rehabilitation technology, and in addition are familiar with the design process.) The main concern that was expressed, besides safety and reliability (which are also general engineering design concerns) is a potential problem with consumer acceptance. Thus (as explained in Section II), we designed a wheelchair with legs as attachments as opposed to walking chairs. The legs were designed so that they could

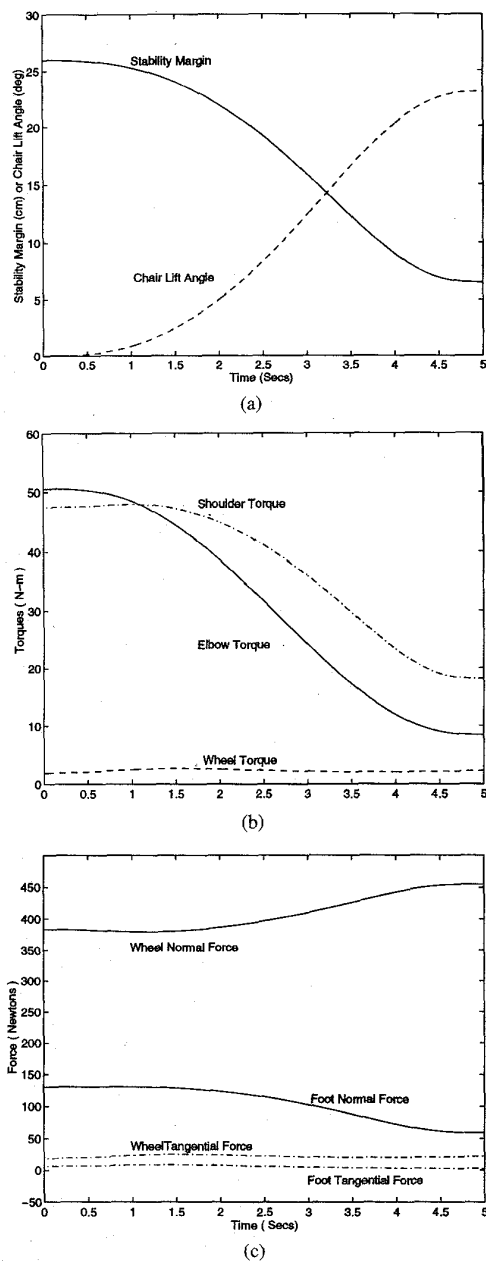


Fig. 16. The results of a computer simulation of the wheelchair with a 75 kg occupant climbing a one foot (0.3048 m) curb: (a) the stability margin (cm) and the tilt of the chair, θ_0 (deg); (b) the torques in Newton-meters encountered at the shoulder/hip (joint 1), the elbow/knee (joint 2), and the wheel; and (c) the normal and tangential foot and wheel forces in Newtons.

be tucked under the chair when not being used. The chair was designed around standard power supplies (12 V batteries) and is compact. While the consumer designers felt it desirable to have a modular design in which it would be possible to easily attach to existing wheelchairs, this was not accomplished in the current design. Our initial attempts to develop such a modular product, and some of the stability related safety problems with this modular design are reported in [25], [26]. There is also a concern relating to how conspicuous the user will feel using such an aid. While this "distractibility factor" depends to a

large extent on the environment and society, it is necessary to make the design more "unrobot-like." Finally, as with all technologies of this nature, there is a concern about the maintenance and reliability of such a device.

An important design issue that is yet unresolved is the user interface for the chair. There is no obvious choice for the best method of control of such a device, although there should be as much user control as can be made compatible with simplicity of operation. The user should have ultimate control over what the device does and when, but he/she should not need the mind/body coordination of a test pilot to complete maneuvers. Although the current control interface is a computer keyboard with a simple menu, we imagine a graphical menu-driven system that is typical of Macintosh or Windows based software. The interface will allow the user to accomplish routine maneuvers easily. At the same time, it will allow the user to explore alternate uses of the technology. For example, the legs can be used for picking items up off the floor, removing obstacles, moving furniture or for reaching into corners.

While the user interface and clinical testing are important directions for future work, the immediate concern relates to user safety and reliability. In the current design, redundant actuation provides for a limp home mode so that the user is not stranded with an awkward, heavy and immobile wheelchair. However, there are no built-in safety mechanisms that protect the user during curb climbing maneuvers. The first task is to design an automatic attitude regulation mechanism that moves the rider forward during climbing maneuvers and back during descents while keeping the chair horizontal. An example of such a device is suggested in [7]. This increases the stability of the system and adds to the comfort of the rider. The second task is to explore the use of a third leg as a crutch to enhance stability and to allow more complex terrains such as stairs. This will provide additional redundancy and make the vehicle safer.

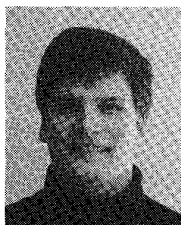
VIII. CONCLUSIONS

We presented the design considerations, optimization and the control of an adaptive mobility system for the disabled. Our prototype has two legs and two powered wheels and uses legs and wheels to locomote. The configuration and dimensions are optimized for traversing obstacles such as steps. The legs are controlled using an impedance control scheme and an active traction optimization scheme distributes the loads between the wheels and legs. The system can walk over obstacles, climb 12 in steps and walk up 30° ramps. It weighs 70 lbs without batteries and payload and to date it has been tested with payloads of up to 150 lbs.

The paper demonstrated the feasibility of the proposed concept and its advantages. While much remains to be done before the prototype can be considered a viable commercial product, this is the first time such a versatile mobility system has been designed, built and successfully tested. Further, the methodology for designing and developing a working prototype is of considerable significance and is being presented here for the first time.

REFERENCES

- [1] R. A. Cooper, M. Macleish, and C. A. McLaurin, "Racing wheelchair roll stability while turning: A simple model," *J. Rehab. Res. Develop.*, vol. 29, no. 2, pp. 23–30, 1992.
- [2] R. A. Cooper, K. J. Steward, and D. P. VanSickle, "Evaluation of methods for determining rearward static stability of manual wheelchairs," *J. Rehab. Res. Develop.*, vol. 31, no. 2, pp. 144–147, 1994.
- [3] H. Funakubo, "Travelling and walking vehicle," Japan Pat. 60-33172, Feb. 1985.
- [4] M. Hiller and A. Kecskemethy, "A computer-oriented approach for the automatic generation and solution of the equations of motion for complex mechanisms," in *Proc. 7th World Congr. Theory of Machines and Mechanisms*, Sevilla, 1987.
- [5] S. Hirose, "A study of design and control of a quadruped walking," *Int. J. Robotics Res.*, vol. 3, no. 2, pp. 113–133, 1984.
- [6] S. Hirose and A. Morishima, "Design and control of a mobile robot with an articulated body," *Int. J. Robotics Res.*, vol. 9, no. 2, pp. 99–114, 1990.
- [7] S. Hirose, T. Sensu, and S. Aoki, "The TAQT carrier: A practical terrain-adaptive quadru-track carrier robot," in *Proc. IEEE/RSJ Int. Conf. Intelligent Robots Syst.*, Raleigh, NC, July 1992, pp. 2068–2073.
- [8] N. Hogan, "Impedance control: Parts I, II," *J. Dynamic Syst., Measurement Contr.*, vol. 107, pp. 1–16, Mar. 1985.
- [9] *Home Care*, Atlanta show products, Atlanta, GA, Nov. 1992.
- [10] T. Houston and R. Metzger, "Combination wheelchair and walker apparatus," U.S. Pat. 5 137 102, Aug. 11, 1992.
- [11] V. Kumar and K. J. Waldron, "Actively coordinated mobility systems," *ASME J. Mechanisms, Transmissions and Automation in Design*, vol. 111, no. 2, pp. 223–231, 1989.
- [12] A. McLaurin and P. Axelson, "Wheelchair standards: An overview," *J. Rehab. Res. Develop. Clinical Suppl.*, vol. 2, pp. 100–103, 1990.
- [13] H. Miura and H. Shimoyama, "Dynamic walk of a biped," *Int. J. Robotics Res.*, vol. 3, no. 3, pp. 60–74, 1984.
- [14] R. S. Mosher, "Exploring the potential of a quadruped," *Int. Automotive Eng. Congr.*, Detroit, MI, Jan. 1969, SAE paper 690191.
- [15] P. D. Nisbet, J. P. Odor, and I. R. Loudon, "The CALL Center smart wheelchair," in *First Int. Conf. Robot. Appl. Med. Healthcare*, Ottawa, Ont. Canada, 1988.
- [16] D. E. Okhotsimski, V. S. Gurfinkel, E. A. Devyanin, and A. K. Platonov, "Integrated walking robot development," in *Machine Intelligence*, J. E. Hayes, D. Michie, and L. J. Mikulich, Eds., 1977, vol. 9.
- [17] E. Peizer and D. W. Wright, "Five years of wheelchair evaluation," Veterans Administration Prosthet. Cen., New York, NY, 1969.
- [18] M. H. Raibert, *Legged Robots that Balance*. Cambridge, MA: M.I.T. Press, 1985.
- [19] M. W. Thring, *Robots and Telechairs: Manipulators with Memory, Remote Manipulators, Machine Limbs for the Handicapped*. New York: Halsted, 1983.
- [20] N. Ulrich, and V. Kumar, "Mechanical design methods of improving manipulator performance," in *Proc. 5th Int. Conf. Advanced Robotics*, Pisa, Italy, June 1991, pp. 515–520.
- [21] H. F. M. Van der Loos, S. J. Michalowski, and L. J. Leifer, "Development of an omnidirectional mobile vocational assistant robot," in *3rd Int. Conf. Assoc. Adv. Rehab. Tech.*, Montreal, P.Q., Canada, June 1988.
- [22] D. R. Voves, J. F. Prendergast, and T. J. Green, "Stairway chairlift mechanism," U.S. Pat. 4 913 264, Apr. 1990.
- [23] H. Wakaumi, K. Nakamura, and T. Matsumura, "Development of an automated wheelchair guided by a magnetic ferrite marker lane," *J. Rehab. Res. Develop.*, vol. 29, no. 1, 1992.
- [24] K. J. Waldron, V. J. Vohnout, A. Pery, and R. B. McGhee, "Configuration design of the adaptive suspension vehicle," *Int. J. Robotics Res.*, vol. 3, no. 2, pp. 37–48, 1984.
- [25] P. Wellman, V. Krovi, and V. Kumar, "An adaptive mobility system for the disabled," *1994 IEEE Int. Conf. Robotics Automation*, May 8–13, 1994, pp. 2006–2011.
- [26] P. Wellman, "A hybrid mobility system," Masters thesis, Dep. Mechanical Eng. and Appl. Mechanics, Univ. Pennsylvania, 1994.
- [27] D. M. Wilson, "Insect walking," *Ann. Rev. Entomology*, vol. 11, pp. 103–122, 1966.
- [28] C.-D. Zhang and S. M. Song, "Gaits and geometry of a walking chair for the disabled," *J. Terramechanics*, vol. 26, no. 314, pp. 211–233, 1989.



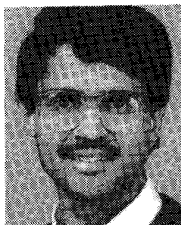
Parris Wellman received the B.S.E. degree in mechanical engineering and applied mechanics and the M.S.E. degree in mechanical engineering from the University of Pennsylvania in May 1993 and December 1994, respectively. He is currently pursuing the Ph.D degree at Harvard University in the division of applied sciences.

His current research involves haptic and vibration displays for virtual environments as well as medical schools.



Venkat Krovi received the B. Tech degree in mechanical engineering from the Indian Institute of Technology in 1992. He is currently pursuing the Ph.D degree in mechanical engineering at the University of Pennsylvania.

His current research interests include dynamics, control, electromechanical systems, and manufacturing, with applications to rehabilitation engineering.



Vijay Kumar received the M.Sc. and Ph.D. degrees in mechanical engineering from The Ohio State University in 1985 and 1987, respectively.

He has been on the faculty in the department of mechanical engineering and applied mechanics at the University of Pennsylvania since 1987. He is currently an associate professor and also holds a secondary appointment in the department of computer and information science. He is currently on the editorial board of the *Journal of the Franklin Institute* and is an associate editor of the *IEEE*

TRANSACTIONS ON ROBOTICS AND AUTOMATION. His research interests include kinematics, robotics, manufacturing, mechanism design, and control.

Dr. Kumar is the recipient of the 1991 National Science Foundation Presidential Young Investigator award.

William Harwin, for a photograph and biography, see the January 1995 issue of this *TRANSACTIONS*, p. 12.